

## Test Method

## Strain distribution in cruciform specimens subjected to biaxial loading conditions. Part 2: Influence of geometrical discontinuities

Ebrahim Lamkanfi<sup>a,\*</sup>, Wim Van Paepegem<sup>a</sup>, Joris Degrieck<sup>a</sup>, Carla Ramault<sup>b</sup>,  
Andreas Makris<sup>b</sup>, Danny Van Hemelrijck<sup>b</sup>

<sup>a</sup> Department of Materials Science and Engineering, Ghent University, Sint-Pietersnieuwstraat 41, 9000 Ghent, Belgium

<sup>b</sup> Department of Mechanics of Materials and Constructions, Free University of Brussels, Pleinlaan 2, 1050 Brussels, Belgium

## ARTICLE INFO

## Article history:

Received 28 August 2009

Accepted 12 October 2009

## Keywords:

Laminate

Strength

Stress concentrations

Finite element analysis

Biaxial

## ABSTRACT

In this paper, the influence of the geometrical design on the strain distribution in cruciform specimens is investigated. It will be shown that geometrical discontinuities, such as the milled zone and the fillet corners which are, respectively, introduced in the cruciform specimen to obtain a more uniform biaxial strain distribution and to guide the loads into the centre zone, result in local high strain concentrations. For this purpose, the digital image correlation technique and the finite element method were employed to trace the origin of these concentrations. It also appeared that the type of load, whether it was applied in a uniaxial or biaxial way, had a minor influence on the observed strain concentrations. The same conclusion could be drawn for the effect of the fibre orientation on the development of these strain intensities. Moreover, this study reveals that the geometrical irregularities lead to complex stress states which make the cruciform specimen fail prematurely. This complicates the determination of the true ultimate biaxial strength of a composite material.

© 2009 Elsevier Ltd. All rights reserved.

### 1. Introduction

From the early seventies, many attempts have been made by several researchers [5,8] to perform biaxial tests on different kinds of polymer composites. Tubular specimens were the earliest geometrical types that were used to obtain a bidirectional stress state. One of the main reasons why alternative geometries were explored for biaxial testing applications was that the use of internal pressure, in combination with axial or torsional forces, led to significant built-up of stresses in the thickness direction [1,2]. The dominant effect of these thickness stresses on the overall stress state of the material indicated that these types of tests could give an insight only into tubular-like

applications such as pressure vessels. Consequently, in other applications where the through-thickness stresses and strains are negligible, flat specimens would be more suitable to obtain more realistic stress–strain relationships and, therefore, also better predictions for failure and strength criteria could be expected. Besides the development of a wide range of loading systems, a variety of cross-shaped geometries have been investigated with always the same and obvious requirement in mind: the load has to be transferred in a proper way to the center zone of the specimen, where the biaxial loading state is intended to be built-up uniformly. The aim of this paper is to present numerical and experimental results describing in detail how this condition of uniform strain distribution in the biaxial characterization of composite materials is affected by discontinuities in the cruciform geometry. First, the design philosophy which has been used by previous researchers will be discussed briefly. This discussion is necessary to position the investigated cross-shaped

\* Corresponding author. Tel.: +32 9 264 95 34.

E-mail addresses: [ebrahim.lamkanfi@ugent.be](mailto:ebrahim.lamkanfi@ugent.be), [elamkanf@gmail.com](mailto:elamkanf@gmail.com) (E. Lamkanfi).

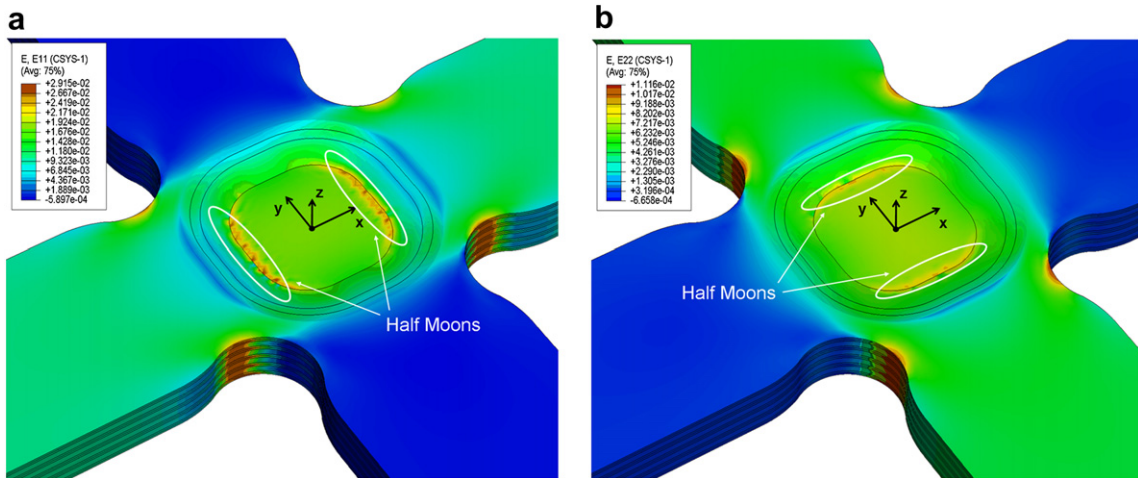


Fig. 1. Half moon pattern in  $x$ -direction (a) and  $y$ -direction (b) loaded specimen.

geometry in the design field. Moreover, an accurate three-dimensional finite element model has been developed to acquire a fundamental insight in the geometrical parameters that affect the load transfer to the center zone and to discuss their consequences on the damage mechanisms. Furthermore, the digital image correlation technique (DICT) is used as a validation method for the numerically obtained surface strains.

## 2. Current cruciform design philosophy

Previous research [4,10] showed that the design requirement of a maximum uniform strain field in the central area of the cruciform forms one of the main difficulties in the biaxial testing of cruciform specimens. The studies also pointed out that, therefore, a general design philosophy for this type of experiment is difficult to obtain. Nevertheless, one can divide the existing geometry types into more or less three main categories: the cut type, the reduced section type and the strip-and-slot type [4]. Whereas in the cut type the rounding radii are used at the intersection of the arms to reduce the load sharing between the arms and, therefore, to increase the load transfer to the centre zone, the reduced section type has the aim of leading the incoming load to the centre zone where damage is expected to start. The strip-and-slot type is mainly used in metallic alloys where it has the purpose of reducing the effect of load sharing between the arms. This latter type will not be a part of the discussion due the difficulties one would face when trying to apply it to composite materials. Therefore, only the effects of a combination of the first two types will be discussed in view of the design requirement mentioned above. The current cruciform geometry studied in this paper belongs to a combination of these two categories [6,7] and is also a variation on the design used by Welsh [9].

## 3. Influence of geometrical discontinuities

It is of great importance to investigate where the strain intensities such as the half moons, which are discussed in

Ref. [3], are actually originating from. As shown there, the mismatch between the three-dimensional obtained surface strains and the digital image correlation results, pointed out that this could only be due to possible cracks at the transition zone between the milled and un-milled area. This was also the case as shown in Fig. 8 of Ref. [3]. In this section a detailed study is presented showing that all strain intensities found in the current cruciform are due to irregularities in the geometrical design. These can be divided in the milled area and the fillet corners. Also, a phenomenon which is called here the strain relieved zone, which is found just behind the central milled area in the highest loading direction, is proven to have an important influence on location of the strain intensities. In the following paragraphs each of these zones is discussed separately.

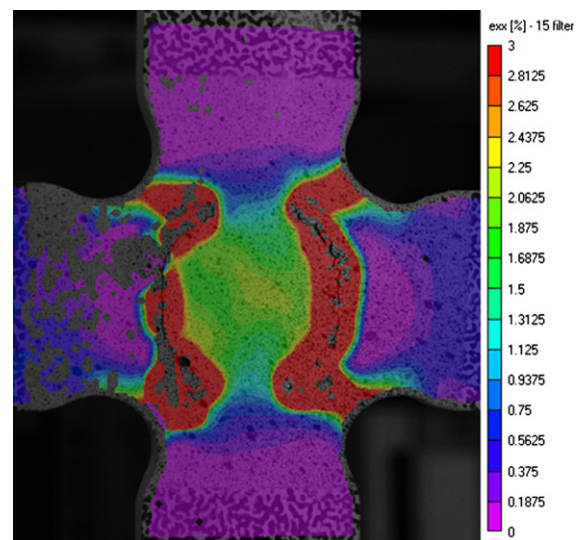
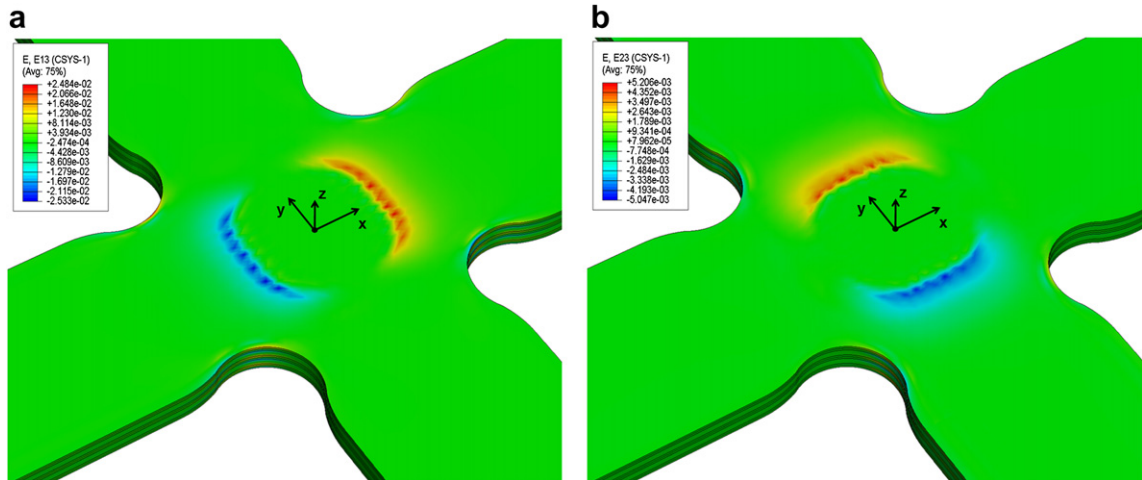


Fig. 2. Cracks initiated at the interface between the skew edges and the flat zone of the milled area. Pulling out of the left hand of the cruciform leads to final failure.



**Fig. 3.** Strains  $\varepsilon_{xz}$  due to  $x$ -direction loading (a) and strains  $\varepsilon_{yz}$  due to  $y$ -direction loading (b). Hereby the three top and bottom layers are disguised.

### 3.1. Milled area

For this zone, the impact of the load direction on the strain intensity is first studied. Two models are, therefore, presented with loads applied in a uniaxial way: one in the  $x$ -direction and the other in the  $y$ -direction. The respective values for the applied stresses, namely  $281.27 \text{ N/mm}^2$  and  $73.059 \text{ N/mm}^2$ , give the same line load magnitudes as those used in the shell model (Ref. [3]) which can be obtained by simply multiplying the stresses with the specimen thickness of  $6.57 \text{ mm}$ . In Fig. 1a and b it can be seen that a half moon pattern is present in both models with the highest values in the  $x$ -direction load case. The implication of these strain concentrations, which start to build up at lower load levels, can be found in Fig. 2 where a DIC image is shown of a uniaxial test performed in the  $x$ -direction at 80% of the biaxial ultimate load. It can be clearly seen that a crack is initiated at the interface

between the skew edges of the milled zone and the flat area of this region. It has to be emphasized that this photograph was taken at a moment where the load is still applied on the arms, which opens the crack and makes it clearly visible. The reason why the crack has not been as clear as shown in Fig. 2 in most of the experiments is believed to be twofold. The first is that for the cases where the specimen was not loaded until the final failure, the paint of the speckle pattern was bridging the crack. This made it impossible to detect the anomaly due to crack closure when the specimen was taken out of the testing machine for inspection. A second reason is that, for the cases where the specimens were loaded until final failure, the brittle behaviour of the glass fiber and the quick follow-up of final failure after crack initiation obstructed the observation of this irregularity. It is, therefore, assumed that Fig. 2 was taken at almost exactly the time of complete failure. When the load is slightly

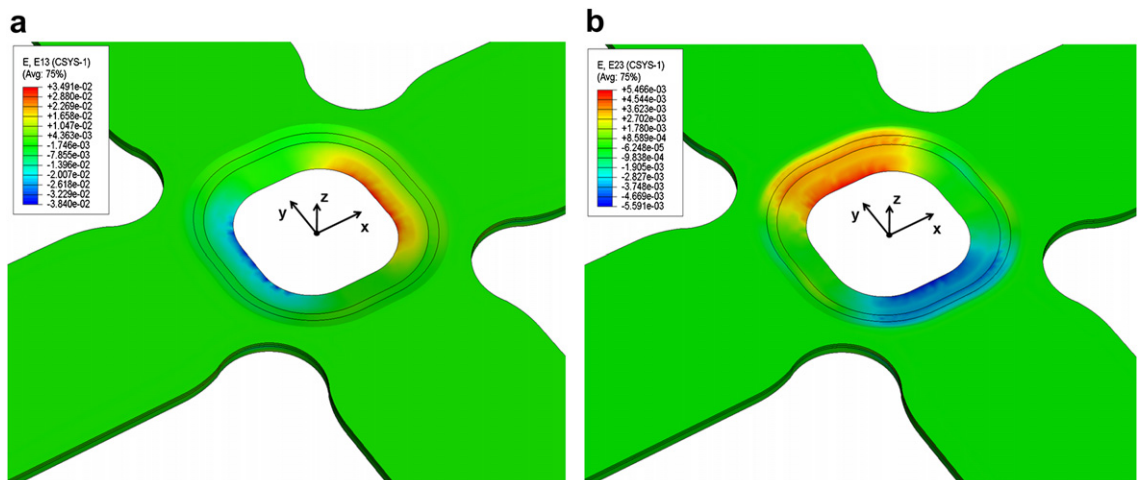


**Fig. 4.** Strains  $\varepsilon_{xz}$  due to  $x$ -direction loading (a) and strains  $\varepsilon_{yz}$  due to  $y$ -direction loading (b). Hereby all the layers are disguised except from the three top layers.

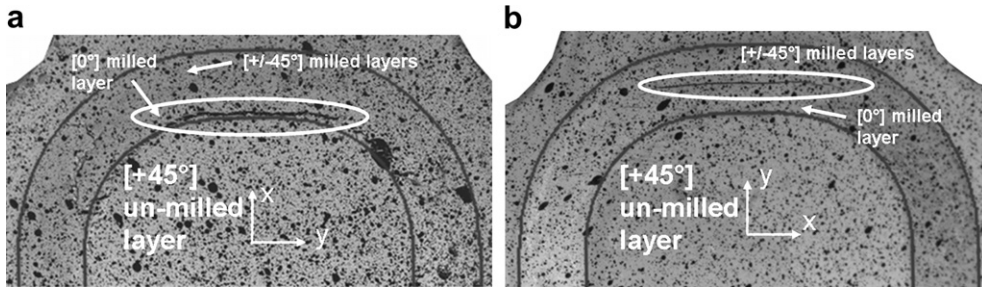


**Fig. 5.** Crack initiation at the [0°] milled layer and the [+45°] un-milled layer for x-direction loading (a). Crack initiation between the milled the [−45°] milled layer and [0°] milled layer for y-direction loading.

increased, a very sudden failure mechanism takes place where the left horizontal part of the specimen is torn out of the rest of the specimen.

Further investigation of the numerical results reveals that the position of the initiation of the crack can be attributed to the presence of the load carrying [0°] fibres, which are also responsible for high values of the inter-laminar strains  $\epsilon_{xz}$  between the first milled [0°] layer and the un-milled [+45°] layer (Fig. 3a). A detailed image of these strains is shown in Fig. 4a, where the highest values are located at the mentioned interface and gradually vanish along the base of the skew edge to the surface of the specimen. It is believed that these effects are the main reasons why the crack is initiated at the interface between the [0°] milled layer and the [+45°] un-milled layer, as shown in the experimental proof of Fig. 5a. In the y-direction case, the loads are primarily transferred through the [±45°] layers leading to a gradual spread of the high inter-laminar strains  $\epsilon_{yz}$  over the entire skew edges in the y-direction. In Fig. 4b it can even be seen that the concentration zone at the discontinuity interface is also redistributed more than in the case of Fig. 4a. This shift leads to the initiation of cracks between the [±45°] milled layers and [0°] milled layer, as found in the experiments (Fig. 5b). Nevertheless, the simulations show that the inter-laminar strains remain high at

the transition between the flat area of the milled area and the skew edges (Fig. 3b). We believe that this is due to the numerical tie, which is just an approximation, and will not take place because the strains will already have been redistributed due to the crack. Moreover, it can be seen in Fig. 6a that just below the milled [0°] layer the  $\epsilon_{zz}$  values are positive, whereas a small distance away from these skew edges in the direction of the central zone they become negative. This  $\epsilon_{zz}$  flip-over also contributes, in the x-direction loading case, to the crack initiation effect. This effect is not occurring in the y-direction loading direction situation (Fig. 6b) where the half moons remain visible, but with magnitudes lower than in the x-loading direction. As mentioned above, this is due to the fact that the load is transferred directly through the [±45°] layers. With this, it is clearly indicated that the load directions are not responsible for the existence of these moons. The same conclusion can also be drawn for the fibre directions, as seen in Fig. 7a, where a pure [0°]<sub>14</sub> lay-up has been simulated. Also, the change of the stacking sequence into a pure [±45°]<sub>7</sub> lay-up does not make the concentrations vanish (Fig. 7b). Therefore, we can conclude that the introduction of the surface discontinuity is responsible for the existence of these half moons at the transition between the skew edges and the flat zone of the milled area.

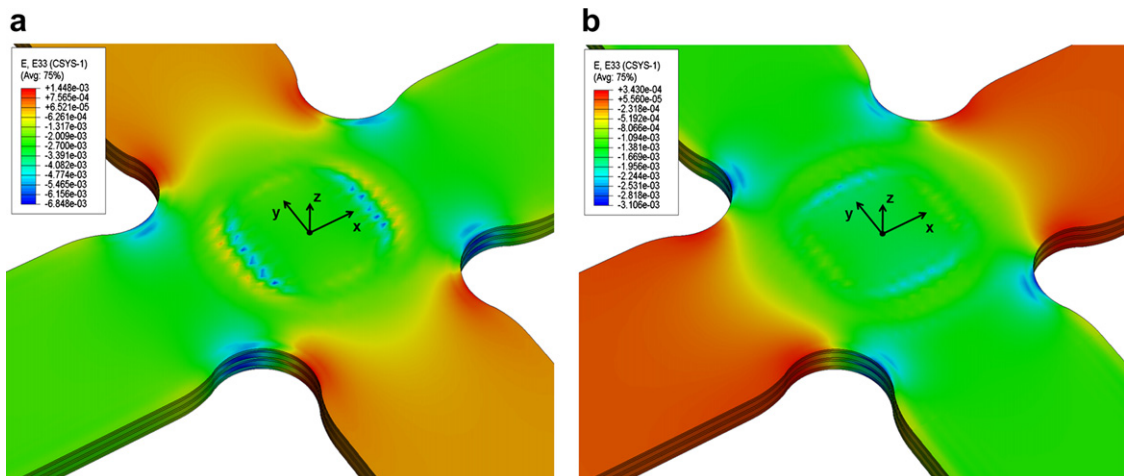


**Fig. 6.** Strains  $\epsilon_{zz}$  due to x-direction (a) and y-direction (b) loading. Hereby the three top and bottom layers are disguised.

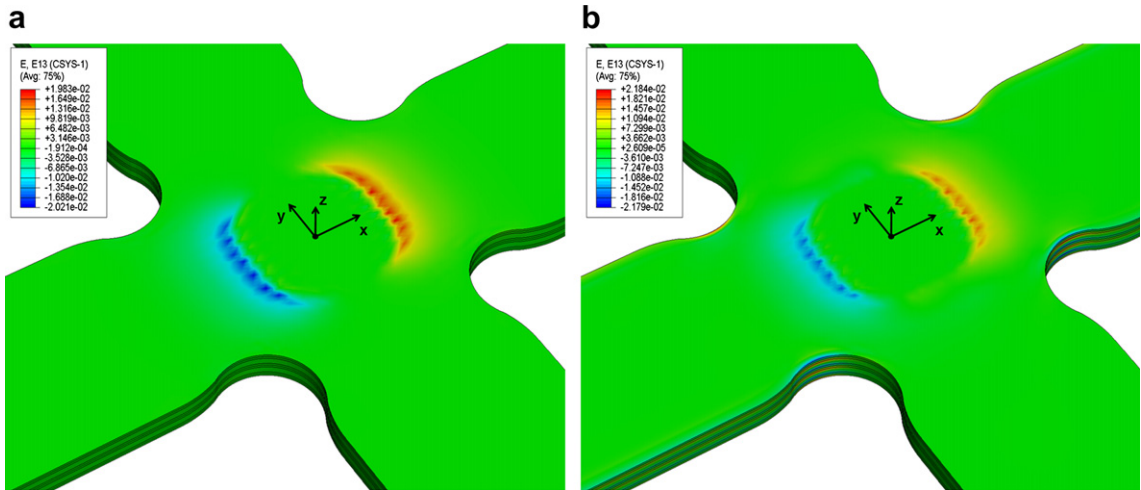


Fig. 7. Influence of the fibre directions on the  $\epsilon_{xz}$  strains :  $[0^\circ]_{14}$  lay-up (a) and  $[\pm 45^\circ]_7$  lay-up (b). Biaxial loading is applied.

3.2. Strain relieved zone

Another phenomenon that marks all the above simulations is the presence of a relief area just outside the milled region in the direction of the highest load. It seems that the load that is introduced in the arms changes its direction and leaves an area of low stresses and strains behind. These relieved areas act as a deviator for the load paths which change their trajectories towards the outer boundaries. Moreover, these zones can be observed through all the layers of the stacking sequence, even in the case of a two-dimensional model (see Ref. [3]) as shown in Fig. 8a. This points out that the phenomenon is caused by in-plane effects. It is, therefore, interesting to notice that these elliptical areas are always formed just at the transition of the two rounding radii that are introduced in the material

to lead the loads into the central area. It appears that just the contrary happens. In the next paragraphs this is proved by disregarding the three top and bottom milled layers due to the aforementioned in-plane effect of these relief areas.

3.3. Rounding radii

As mentioned above, it is seen from the simulations that the load trajectories are deviated towards the corners, resulting in strong stress and strain concentrations in the vicinity of the transition zone between the inner circle and the outer rounding circle. From there the load is then principally transferred to the centre zone, leaving the relieved zone behind. This can be clearly seen in Fig. 8b. Moreover, when the deformation scale factor is increased in the finite element models, a new phenomenon appears:

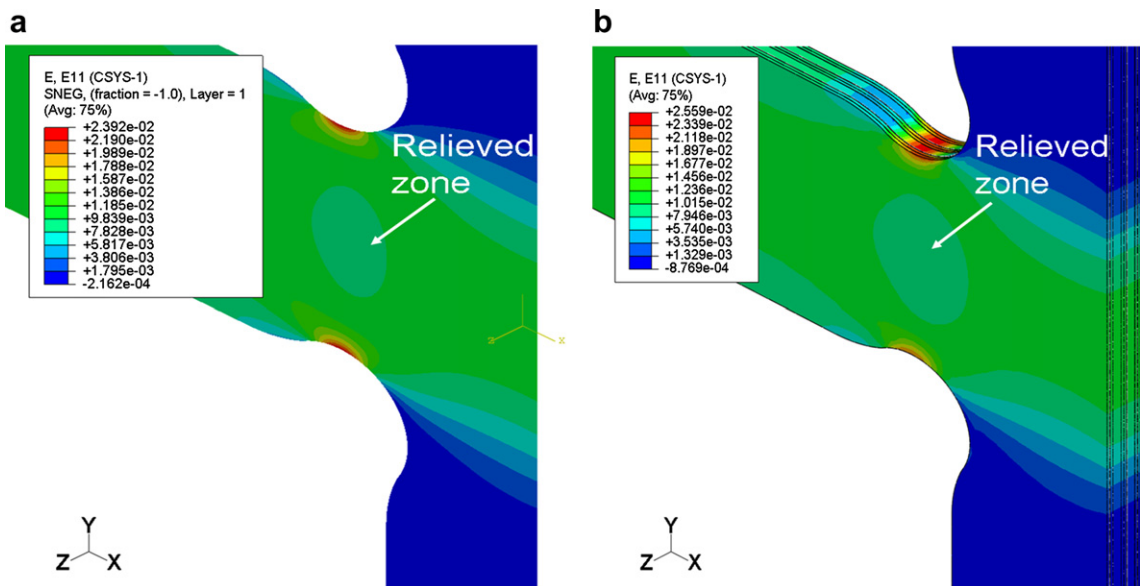
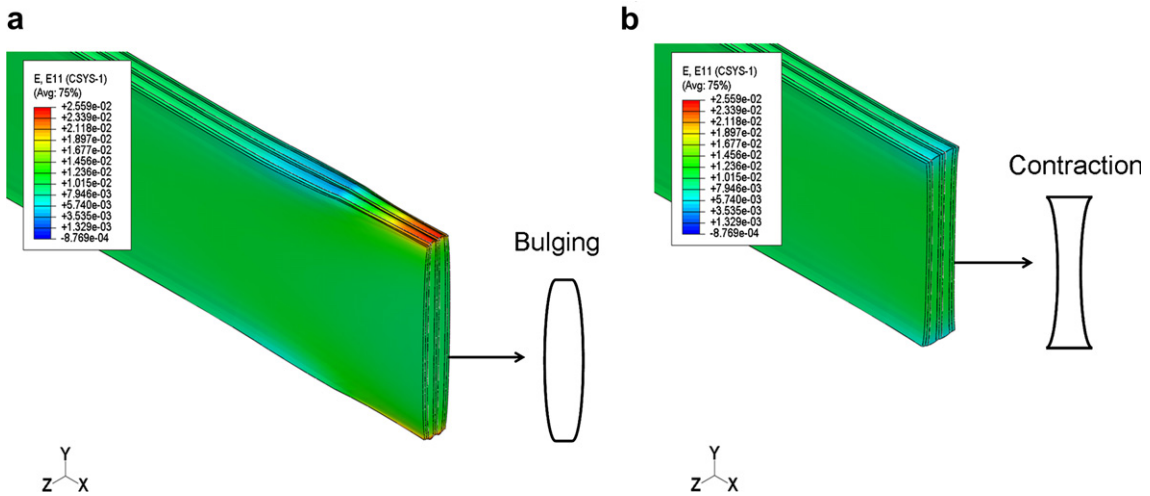
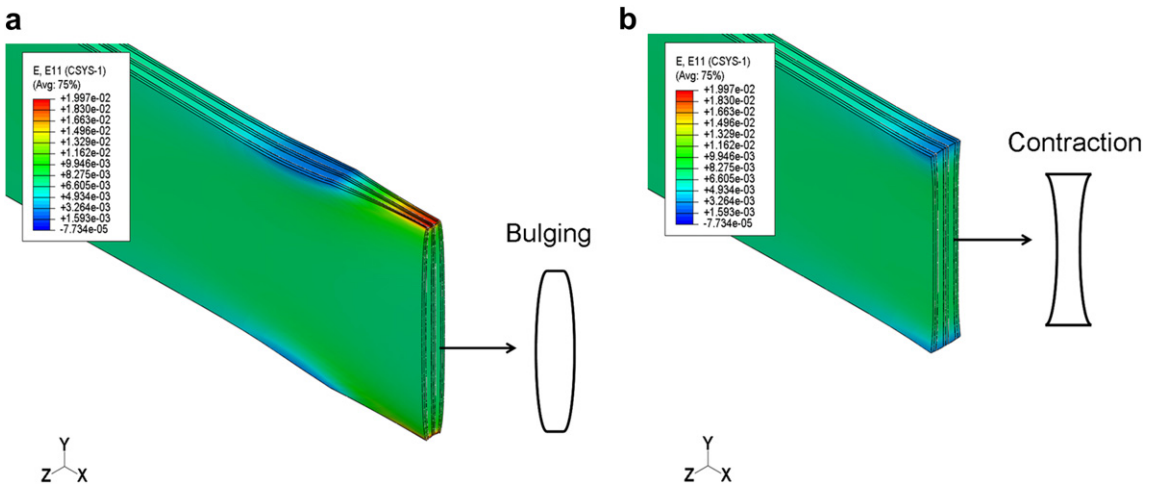


Fig. 8. Relieved area in between the two corner radii : the two-dimensional case (a) and the three-dimensional model (b).



**Fig. 9.** Strains  $\varepsilon_{xx}$  in  $[\pm 45^\circ/0^\circ]$  lay-up model without milled layers at the inner (a) and the outer (b) rounding circle in a  $x$ -direction loading case. Bulging (a) and contraction (b) effect is respectively shown.



**Fig. 10.** Strains  $\varepsilon_{xx}$  in a pure  $[0^\circ]$  lay-up model without milled layers at the inner (a) and the outer (b) rounding circle. Bulging (a) and contraction (b) effect is respectively shown.

at the transition zone between the inner and outer circle (detailed Fig. 2 found in [3]), the cross-section of the arm changes respectively from a bulged (Fig. 9a) to a contracted (Fig. 9b) form. This could be a possible reason why the introduced loads in the arms are deviated towards the rounding radii, leading to the existence of the high strain intensity zones in those areas. Furthermore, this effect is observed irrespective of the load direction and the fibre orientation of the material. This is confirmed by simulations depicted in Fig. 10a and b where all the layers are changed to  $[0^\circ]$  layers. Even in the case where the material properties of the cruciform are changed into those of an isotropic material, the concentrations at the corner radii remain unchanged. The contraction and bulging effect also holds in the case where the load direction is changed from the  $x$ -direction (Fig. 9a and b) to the  $y$ -direction on the  $[\pm 45^\circ/0^\circ]$  stacking sequence model without milled layers.

Therefore, it can be concluded that, besides the milled area, the rounding radii also disturb the load transfer in a significant way, leading to the initiation of the first cracks, as shown in Figs. 4 and 5.

#### 4. Conclusions

In this paper, the influence of geometrical discontinuities on the strain distribution in biaxially loaded specimens is studied. A mixed experimental numerical approach, based on the finite element method and the digital image correlation technique, showed that the mismatch in strain values is due to the existence of a crack at the transition zone between the central milled and surrounding un-milled area. It is also proven that these strain concentrations are independent from the load direction and the type of load, leading to the only remaining option that the milling out

itself is responsible for these strain concentrations. Furthermore, it is found that the existence of a relieved zone in the direction of the highest load, just behind the milled area, diverts the incoming load trajectories to the corners, resulting also in high intensity zones there. It can, therefore, be concluded that these geometrical discontinuities have a major influence on the strain distribution, inducing the cruciform to fail prematurely before the ultimate biaxial strength is reached.

### Acknowledgements

The authors gratefully acknowledge the financial support for this research by the Fund for Scientific Research – Flanders (FWO).

### References

- [1] M.F.S. Alkhalil, P.D. Soden, R. Kitching, M.J. Hinton, The effects of radial stresses on the strength of thin-walled filament wound GRP composite pressure cylinders. *International Journal of Mechanical Sciences* 38 (1) (1996) 97–120.
- [2] V.K.S. Choo, D. Hull, Influence of radial compressive stress owing to pressure on the failure modes of composite tube specimens. *Journal of Composite Materials* 17 (4) (1983) 344–356.
- [3] E. Lamkanfi, W. Van Paepegem, J. Degrieck, C. Ramault, A. Makris, D. Van Hemelrijck, Strain distribution in cruciform specimens subjected to biaxial loading conditions. Part 1: two-dimensional versus three-dimensional finite element model. *Polymer Testing* 29 (1) (2010) 7–13.
- [4] Y. Ohtake, S. Rokugawa, H. Masumoto, Geometry determination of cruciform-type specimen and biaxial tensile test of C C composites. *High Temperature Ceramic Matrix Composites Iii* 164-1 (1999) 151–154.
- [5] V.D. Protasov, V.P. Georgievskii, Anisotropy of the strength properties of reinforced plastics. *Mechanics of Composite Materials* 3 (3) (1967) 308–311.
- [6] A. Smits, D. Van Hemelrijck, T.P. Philippidis, A. Cardon, Optimization of a cruciform test specimen for biaxial loading of fiber reinforced material systems, in: *Proceedings of 11th European Conference on Composite Materials*, Rhodes, Greece, 2004.
- [7] A. Smits, D. Van Hemelrijck, T.P. Philippidis, A. Cardon, Design of a cruciform specimen for biaxial testing of fibre reinforced composite laminates. *Composites Science and Technology* 66 (7–8) (2006) 964–975.
- [8] H. Thom, A review of the biaxial strength of fibre-reinforced plastics. *Composites Part A-Applied Science and Manufacturing* 29 (8) (1998) 869–886.
- [9] J.S. Welsh, D.F. Adams, An experimental investigation of the biaxial strength of IM6/3501-6 carbon/epoxy cross-ply laminates using cruciform specimens. *Composites Part A-Applied Science and Manufacturing* 33 (6) (2002) 829–839.
- [10] Y. Yu, M. Wan, X.D. Wu, X.B. Zhou, Design of a cruciform biaxial tensile specimen for limit strain analysis by FEM. *Journal of Materials Processing Technology* 123 (1) (2002) 67–70.